Journal of Power Sources 269 (2014) 403–411

Contents lists available at ScienceDirect

Journal of Power Sources

journal homepage: www.elsevier.com/locate/jpowsour

Reducing start-up time and minimizing energy losses of Microbial Fuel Cells using Maximum Power Point Tracking strategy

Daniele Molognoni [a, b, *], Sebastià Puig [b], M. Dolors Balaguer [b], Alessandro Liberale [c], Andrea G. Capodaglio [a], Arianna Callegari [a], Jesús Colprim [b]

[a] Department of Civil Engineering and Architecture (D.I.C.Ar.), University of Pavia, Via Ferrata 1, 27100 Pavia, Italy
[b] Laboratory of Chemical and Environmental Engineering (LEQUiA), Institute of the Environment, University of Girona, Campus Montilivi s/n, Facultat de Ciencies, E-17071 Girona, Spain
[c] Power Electronics Laboratory, Department of Electrical, Computer and Biomedical Engineering, University of Pavia, Via Ferrata 1, 27100 Pavia, Italy

HIGHLIGHTS

- A Maximum Power Point Tracking system was studied to optimize MFC power generation.
- Pig wastewater was used as anode fuel to evaluate the system under real conditions.
- External load control decreased MFC start-up time of about one month.
- External load control increased Coulombic efficiency and decreased energy losses.

ARTICLE INFO

Article history:
Received 20 May 2014
Received in revised form
23 June 2014
Accepted 5 July 2014
Available online 11 July 2014

Keywords:
Coulombic efficiency
Internal resistance
Maximum Power Point Tracking
Microbial fuel cell
Start-up

ABSTRACT

Microbial Fuel Cells (MFCs) are considered to be an environmental friendly energy conversion technology. The main limitations that delay their industrialization include low current and power densities achievable and long start-up times. Maximum Power Point Tracking (MPPT) has been proposed as a method to enhance MFCs electrical performances. However, the specialized literature is still lacking of experimental works on scaled-up reactors and/or real wastewater utilization. This study evaluates the impact of a MPPT system applied to MFCs treating swine wastewater in terms of start-up time and long-term performance. For this purpose, two replicate cells were compared, one with applied MPPT control and one working with fixed resistance. Both MFCs were continuously fed with swine wastewater to validate the control system under real and dynamic conditions. The study demonstrated that the automatic resistance control was able to reduce the start-up time of about one month. Moreover, MPPT system increased of 40% the Coulombic efficiency at steady-state conditions, reduced energy losses associated with anode and cathode reactions and limited methanogenic activity in the anode chamber. A power density of 5.0 ± 0.2 W m^{-3} NAC was achieved feeding the system at an organic loading rate of 10 kg COD m^{-3} d^{-1}.

1. Introduction

Fuel cells are power sources that use catalytic oxidation reactions without resorting to thermal processes, thus achieving direct conversion of chemical energy (of a generic fuel) into electrical energy. In particular, Microbial Fuel Cells (MFCs) directly convert the chemical energy contained into an organic bio-convertible substrate into electrical energy, through the mediation of exoelectrogenic bacteria that act as catalysers of the half-reaction of substrate oxidation [1].

When wastewater is used as anode fuel, MFCs perform wastewater treatment while recovering energy, thus leading to the possibility of energy-producing wastewater treatment plants [2]. Low power density and restricted output voltage of MFCs currently limit their industrial application [3]. Many approaches have been explored to enhance the performances of exoelectrogenic bacteria, to accelerate their growth and to decrease the start-up time needed. These include selection of the inocula [4], electrode

* Corresponding author. Department of Civil Engineering and Architecture (D.I.C.Ar.), University of Pavia, Via Ferrata 1, 27100 Pavia, Italy. Tel.: +39 0382 985592; fax: +39 0382 985589.
E-mail addresses: daniele.molognoni@unipv.it, daniele.molognoni@gmail.com (D. Molognoni).

http://dx.doi.org/10.1016/j.jpowsour.2014.07.033
0378-7753/

potential poisoning [5] and variations in load resistance [6]. Another alternative, not yet fully exploited, is to enhance MFCs power output by controlling the electrical load to always produce the maximum power output [7]. The maximum power, as in any other electrical power source, is drawn when the external resistance (R_{ext}) equals the internal resistance (R_{int}) of the system [8]. More than 50% of the power can be lost if the electrical load is not matched with the internal resistance [7]. Hence external resistance should be (at least) periodically adjusted in order to follow the Maximum Power Point (MPP) [9].

Several Maximum Power Point Tracking (MPPT) methods have been proposed in the literature. One class of MPPT methods uses a mathematical model of the system to compute its impedance (internal resistance in case of direct current) [7,9]. The main problem of such an approach is its complexity and the amount of parameters to calibrate. Another class of methods is represented by non-model based, real-time optimization methods, mainly studied for fast dynamic systems. A real-time optimization method can be used to adjust the value of MFC external resistance, in order to maximize the electrical power delivered at each moment [7]. The R_{ext} control could represent an important requirement in case of wastewater treatment application of MFCs, since the influent quality and the plant operational parameters could vary over daily and/or seasonal basis [10,11].

The first study about MPPT control application to MFCs was carried out by Woodward et al. (2010). They applied and compared different MPPT methods for tracking optimal R_{ext} in two replicate MFCs fed with acetate [7]. In particular, they tested a Perturbation and Observation method (*P*/*O*) and a Gradient method (*G*) for the optimization of individually working cells, plus a Multiunit Optimization method (MU), useful in case of stacked MFCs (fully described in Ref. [12]). The authors concluded that *G* method, even if (in theory) it converged faster than *P*/*O*, was difficult to set up and did not ensure stable performances. On the other hand, *P*/*O* method was easy to tune and showed robust operation. Pinto et al. (2011) [10] tested again the *P*/*O* method on MFCs fed with acetate, and studied the control system performance during long-term operation. They found out that the load-controlled MFC exhibited higher current density and Coulombic efficiency compared to uncontrolled cells, and shorter start-up time (less than 10 days). Moreover, MPPT control application limited MFC methane production during the start-up phase [10,13]. Degrenne et al. (2012) tested a different algorithm to control the external resistance of MFCs [14]. The new algorithm was able to impose a cell voltage equal to one-third of the Open Circuit Voltage (value approximately corresponding to the MPP) but did not show significant advantages with respect to the *P*/*O* method. Boghani and coworkers (2013) [15] tested another MPPT system based on a parsimonious gradient based method (fully described in Ref. [11]). They coupled it with an additional start-up routine, able to poise the anode potential until the current sourced from the MFC did not exceed a certain threshold (method called PP-MPPT). This approach was able to reduce MFC start-up time of about 3 weeks, improving exoelectrogenic bacteria selection and activity (increasing the Coulombic efficiency), avoiding power overshoot during the biofilm enrichment period [16,17] and reducing methanogenesis in the anode compartment. However, the MPPT system alone exhibited similar benefits to the more complex PP-MPPT [15]. It appeared to be better (and easier) to follow directly the MFC internal resistance behavior, and hence MPP variations, with respect to poise the anode potential to values that could be unsustainable for early-stage biofilms.

Automatic resistance control was proven to influence also the exoelectrogenic microbial community composition [6,9,11,13,18] and abundance. Premier et al. (2011) observed that the biomass present in a load-controlled MFC was less than half that in a replicate cell equipped with a static resistance [11]. On the other hand, the power output did not seem to be affected by any control system until the applied resistance remained near the optimal value [5,15,18].

All these results demonstrated the advantages of using a MPPT system to control the current sourced from MFCs. In particular, the *P*/*O* method seemed to be the best compromise between precision, robustness and easy implementation [7]. The automatic resistance control certainly represents a step towards the industrialization of the MFC technology, but still today the specialized literature is lacking of experimental works on scaled-up reactors and/or real wastewater utilization. This paper aims to start filling the gap, offering a comparison between two replicate MFCs, one with the MPPT control applied and one acting as reference cell, equipped with a fixed resistance. Continuously fed swine wastewater was used as anode substrate, in order to evaluate the system under real and dynamic conditions, from an industrial-oriented point of view. Very few studies in the literature demonstrated the feasibility of animal wastewater treatment and bioenergy production using MFCs [19,20].

A complete assessment was carried out in terms of power produced, current intensity, internal resistance, energy losses distribution, organic matter removal and Coulombic efficiency. The effects of MPPT control application were evaluated at short-term and long-term conditions.

2. Materials & methods

2.1. Experimental setup

Two replicate MFCs were operated under different electrical load conditions to evaluate the effects of a MPPT system on their bioelectrochemical performances. In particular, one MFC was subjected to the MPPT algorithm (MPPT-MFC) for automatically controlling the electrical load applied, while the other one was equipped with a fixed external resistance of 30 Ω (Ref-MFC). This resistance value was chosen in order to be near to the static internal resistance of the MFC, based on previous experience gained on similar working cells [21].

The MFCs were constructed using a previously described design [22], and consisted (each one) of an anode and a cathode placed on the opposite sides of a single methacrylate rectangular chamber. The anode and cathode chambers were filled with granular graphite (model 00514, diameter 1.5–5 mm, EnViro-cell, Germany), which decreased the volumes to 370 ± 10 mL net anodic compartment (NAC) and 410 ± 10 mL net cathodic compartment (NCC) respectively. The electrodes were previously washed in 1 M HCl and 1 M NaOH to remove possible metal and organic contamination. Two thinner graphite rods electrodes (250 × 4 mm, Sofacel, Spain) were introduced in each chamber to allow an external electrical connection to the system. An Anion Exchange Membrane (AMI-7001, Membranes International Inc., USA) was placed between the anode and cathode frames. The AEM membrane was chosen because of its lower internal resistance and diffusivity to oxygen, that should allow to achieve higher power densities and Coulombic efficiencies [23].

Swine wastewater from the Food and Agricultural Research Institute (IRTA) of Monells (Girona, Spain) was used as anode fuel. The liquor was stored in a refrigerated tank to promote solids settling and to preserve the organic matter content. The swine wastewater was continuously fed to the anode at a flow-rate of 1.5 L d^{-1}. The cathode was fed, at the same flow-rate, with an oxygen-saturated mineral medium with the following characteristics: 122 mg L^{-1} $NaHCO_3$, 7.6 mg L^{-1} NH_4Cl, 300 mg L^{-1}

$NaH_2PO_4 \cdot 2H_2O$, 1.4 mg L^{-1} $CaCl_2$, 9 mg L^{-1} $MgSO_4 \cdot 7H_2O$, 1.3 mg L^{-1} KCl, 150 mg L^{-1} $KH_2PO_4 \cdot 2H_2O$ and 0.01 mL L^{-1} microelements solution.

Internal recirculation loops (170 L d^{-1}) in each compartment maintained well-mixed conditions and minimized concentration gradients. The temperature of the system was kept constant at 21 ± 1 °C. The anode potential of each MFC was monitored with an Ag/AgCl reference electrode (+197 mV vs Standard Hydrogen Electrode, model RE-5B, BASI, United Kingdom). Anode potentials and overall cell potentials were recorded at 5-min intervals by means of 4 on-line multimeters (Alpha-p, Ditel, Spain) with a data acquisition system (Memograph® M RSG40, Endress + Hauser, Germany). Cathode potentials were calculated by summing the respective MFC anode potential and cell potential.

2.2. MFCs operation

The anode and cathode chambers of both MFCs were inoculated with a mixture of: aerobic activated sludge from the municipal wastewater treatment plant of Girona (20%), anode effluent from a parent MFC performing carbon and nitrogen removal (10%), swine wastewater (10%) and tap water (60%). In the inoculum solution of the anode chambers also 2-bromoethanesulfonate (BES) was added (in concentration of 9.5 mM), in order to inhibit methanogenic microorganisms growth at the beginning of the study [13]. Inoculation was performed in closed electric loop mode, adopting an external resistance of 30 Ω for both the MFCs, and maintaining a recirculation flow-rate of 86 L d^{-1} to promote bacteria fixation at the electrodes surface. This start-up approach (closed electric loop mode) was chosen to facilitate the electron transfer process and thus provide growth advantages for exoelectrogenic bacteria, against proliferation of a methanogenic population. A similar strategy was adopted by Pinto et al. (2011) [10] and corroborated by computer simulations using a MFC model [9]. After 4 days from inoculation, both cells started to be fed continuously and MPPT control was switched on in the controlled cell. This means that, meanwhile Ref-MFC continued to work at an electric load of 30 Ω, the external resistance of MPPT-MFC was let free to vary as to reach and follow the MPP. Anode influent was replaced with fresh one every 5 days, to limit external organic matter degradation and maintain almost constant organic loading rate. Anode and cathode influent conductivities were maintained at equal values (2.7 ± 0.3 mS cm^{-1}) by addition of $NaHCO_3$ to the catholyte. Both the MFCs were fed at a high anode organic loading rate (hereafter OLR) of 10.5 ± 0.7 kg COD m^{-3} d^{-1} for the first 7 weeks of the experiment (first period). At day 53rd the OLR was decreased of 50% to reach a new value of 5.2 ± 0.1 kg COD m^{-3} d^{-1}. The MFCs were fed at this OLR for other 3 weeks (second period). This perturbation was set up in order to evaluate the MPPT control applicability under dynamic conditions.

2.3. Maximum Power Point Tracking system

2.3.1. Hardware description

The experimental set-up used to apply the MPPT control system to the MPPT-MFC is shown in Fig. 1. It consisted of a potentiometers array, which imposed the resistance to the MFC, an amperometer and a voltmeter (Model 2000 $6^1/_2$-Digit Multimeter, Keithley Instruments, USA), that measured current and voltage respectively, and a computer for data elaboration and control of the potentiometers.

The potentiometer used (Intersil X9C102, Future Electronics, UK) was a digitally controlled (XDCP) potentiometer. The device consisted of an array composed of 99 resistive elements and a switching network that mimicked the behavior of the wiper in a classical potentiometer. The available resistance range was from 30 to 1000 Ω in 100 steps. In this specific application the Intersil X9C102 was used as a two-terminal, variable resistor. The position of the wiper element was controlled by the computer: at any given moment the software could command to the potentiometer to change its resistive value by one step (up or down). Since the MFC internal resistance was expected to be in the order of tens of Ohm, 5 potentiometers were connected in parallel. In the resulting configuration the controlled resistance could be selected in a range from 6 to 200 Ω, with a step between two following values of about 2 Ω.

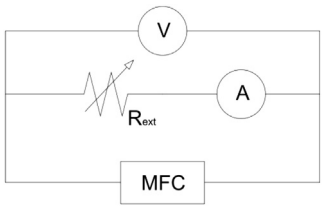

Fig. 1. Experimental set-up used for MPPT control application to MFCs. R_{ext} represents the array of potentiometers, *A* the amperometer and *V* the voltmeter.

2.3.2. Software description

The technique implemented in the software can be classified as a *P*/*O* method. Basically the algorithm was composed of a loop that periodically measured the MFC output power (every 2 min). The value calculated at one iteration (step n_i) was compared to the one measured in the previous iteration (step n_{i-1}): if P_i was bigger than P_{i-1}, the algorithm varied the resistance in the same direction as in the previous step; if P_i was smaller than P_{i-1} the control moved in the opposite direction. Every time a resistance variation was applied, the software allowed the MFC to complete the resulting transient and reach a new stable operation point. This was obtained by continuously monitoring the slope of the output voltage and waiting for it to reach zero (with tolerance of 0.5 mV min^{-1}). Only when the transient was over, a new value of output power was calculated and one iteration was completed. The repetition rate of the iterations was not strictly constant as it depended on the time required by the MFC to settle down to the new working condition. As for all the *P*/*O* algorithms, the real MPP was never actually reached and maintained, but the system continued to oscillate around it [7,10]; nevertheless, with the resolution allowed by the 5 potentiometers in parallel, this oscillation was negligible (0.03 ± 0.04 mW).

2.4. Analysis and calculations

Samples for the determination of total and soluble quotes of Chemical Oxygen Demand (COD_t, COD_s) and 5-day Biochemical Oxygen Demand (BOD_t, BOD_s) were taken at regularly basis from the anode influent ($_{IN}$) and effluent ($_{EFF}$) streams, and analysed with standard wastewater methods [24]. The OLR was calculated (for each MFC) as the daily influent organic matter concentration (in terms of COD_t) divided by the hydraulic retention time. The organic matter removal efficiency (η_{COD_t}, expressed as percentage) was determined with the following equation:

$$\eta_{COD_t} = (COD_{t,IN} - COD_{t,EFF})/COD_{t,IN} \cdot 100 \quad (1)$$

pH and conductivity were measured two times a week for both anode and cathode influents and effluents (pH-Meter BASIC 20^+, EC-Meter BASIC 30^+, Crison Instruments, Spain).

Current (I) and power (P) were retrieved from the cell voltage measurement (V) by application of Ohm's law, concerning the Ref-MFC where external resistance was fixed at 30 Ω. In the case of MPPT-MFC (variable external resistance), current intensity was measured together with cell voltage and the power was easily obtained by $P = I{\cdot}V$. Applied external resistance (R_{ext}) was again calculated by means of Ohm's law ($R_{ext} = V/I$). Polarization curves were periodically performed using a potentiostat (model SP50, BioLogic, France) and by imposing a linear potential decrease of 0.5 mV s^{-1} from the Open Circuit Voltage (hereafter OCV) to a cell voltage of 0 mV, followed by a linear voltage increase of 0.5 mV s^{-1} of the cell voltage to the original OCV. Internal resistance was calculated from the polarization curves, by means of the power density peak method [8].

Anode Coulombic efficiency (CE) was calculated according to Logan et al. [25] using daily average data of current intensity and flow-rate. Organic matter removal term, necessary for the calculation of the maximum theoretical current (denominator of the formula), was estimated in 2 different ways based on the data of COD_s and BOD_t.

2.5. Energy losses distribution

Identifying the limiting factors in MFCs operation is critical for further enhancing their performances. Direct current analytical methods, such as polarization curves, can be used to measure the total internal resistance, but not the resistance of the individual components. There is substantial need for the development of a common method to analyze the quantitative contribution of anode, cathode, membrane and electrolyte resistances to the overall internal resistance [26]. As to complete the electrochemical comparison between Ref-MFC and MPPT-MFC, energy loss factors were calculated, in relation to the two experimental periods performed, from the energy balance equation (Eq. (2)) [27].

$$E_{cell} = E_{emf} - \eta_{An} - \eta_{Cat} - E_{ionic} - E_{\Delta pH} - E_T \quad (2)$$

where the parameters are as follows: E_{cell} (cell voltage), E_{emf} (overall cell electromotive force), η_{An} (anode overpotential), η_{Cat} (cathode overpotential), E_{ionic} (ionic loss), $E_{\Delta pH}$ (pH gradient loss) and E_T (transport loss).

E_{emf} represents the maximum theoretic voltage that can be extracted from the MFC. It was calculated at the initial pHs of the anolyte and catholyte using the Nernst equation, assuming acetate oxidation reaction at the anode and oxygen reduction at the cathode [25]. An equivalent acetate concentration (in mol L^{-1}) was retrieved from the COD_s concentration data of the anode influent. Anode and cathode overpotentials were also calculated by means of the Nernst equation, using effluent values of pH and COD_s (for the anode), and measured values of the electrodes potential (daily averages). E_{ionic} is related to the electrolyte resistance of anolyte and catholyte [28]. It was calculated at both sides of the membrane according to Sleutels et al. [27], with a distance between the membrane and the electrode of 1 cm and a membrane area of 400 cm^2. Daily average data of current intensity were used, and effluent values of electrolytes conductivity. $E_{\Delta pH}$ represents the potential loss related to the pH gradient developing over the membrane during MFCs operation. It was determined by means of Nernst equation, using effluent values of electrolytes pH and rendering a potential loss of −0.059 V per pH unit [22,27]. Following the methodology of Sleutels et al. [27], the ohmic losses other than ionic losses of the electrolytes were not measured and were included in the overpotentials of the anode and the cathode. Finally, the membrane transport loss E_T was calculated from all other potential losses using Eq. (2). The measured cell voltage (E_{cell}) of each MFC was the remaining portion of electromotive force voltage once overcome all the thermodynamic and internal potential losses represented in Eq. (2) [29].

As energy efficiency in MFCs is represented by the product of Coulombic efficiency and voltage efficiency [29], the calculated values of overpotentials were compared with the current intensity production of each cell. A term of resistance related with each energy loss component was calculated from the potential losses according to Ohm's law ($R = V/I$) [28,29]. In this way it was possible to summarize the informations related to the overpotentials analysis and the current intensity generation into a single (resistive) value.

3. Results

3.1. Power generation

Power generated by Ref-MFC and MPPT-MFC during the experimental period (11 weeks) is presented in Fig. 2. This figure reports the applied external resistance (R_{ext}) and the punctual values of internal resistance (R_{int}) calculated from polarization curves analysis.

Inoculation procedure was deployed at day 1st under closed electric loop conditions. After 3 days the MFCs started to be fed in continuous mode, and the MPPT control system was activated for

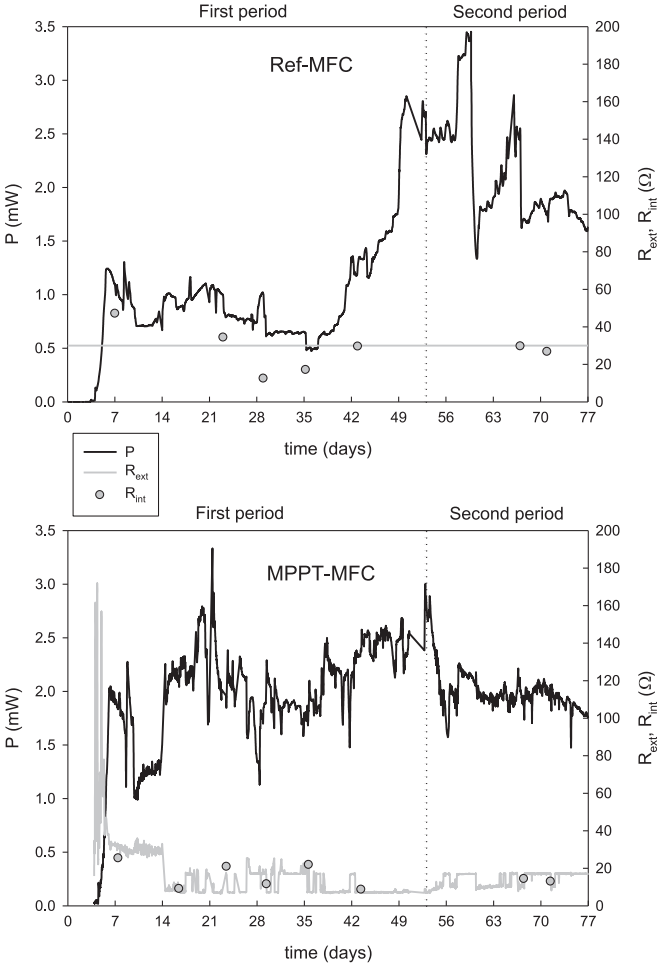

Fig. 2. Power production (P), applied external resistance (R_{ext}) and calculated internal resistance (R_{int}) for Ref-MFC and MPPT-MFC over studied time. Vertical bar represents the organic loading rate variation.

the MPPT-MFC. In less than one day (day 4th from inoculation) both the cells started to generate power, but at different rates. MPPT-MFC reached 2 mW in about 2 days (rate of 1 mW d^{-1}), while in the same time Ref-MFC reached 1.2 mW (rate of 0.6 mW d^{-1}). At day 7th the first polarization curves were performed to both the cells, verifying how the internal resistance of MPPT-MFC (25.3 Ω) was about half the value of Ref-MFC (47 Ω) and how the MPPT system was effectively able to match R_{int} and R_{ext}.

Ref-MFC performed then a stable power production (0.8 ± 0.2 mW) until day 35th, when it started increasing at a rate of 0.1 mW d^{-1} until reaching 2.8 mW at day 52nd. Internal resistance of Ref-MFC, measured at day 43rd, was equal to 29.5 Ω, close to the value of 30 Ω chosen as fixed external resistance. On the other hand, MPPT-MFC external resistance was stable on 30 ± 2 Ω from day 7th to day 14th, meanwhile power production reached 1.4 ± 0.3 mW, value 75% higher with respect to that of Ref-MFC. At day 15th the external resistance dropped down to 9 ± 2 Ω, until day 17th, and the power increased to 2.1 ± 0.1 mW. From this point, external resistance values started oscillating between 6.5 and 25.5 Ω until day 38th. The MFC produced an average power of 2.0 ± 0.3 mW, more than double with respect to the power generated by Ref-MFC in the same period. From day 38th to day 53rd MPPT-MFC showed stable external resistance of 8 ± 2 Ω and a power generation of 2.3 ± 0.2 mW. Internal resistance values always showed good agreement with the one applied by the MPPT control system.

At day 53rd the OLR was decreased from 10 to 5 kg COD m^{-3} d^{-1}. The perturbation was set up to evaluate the MPPT control applicability under dynamic conditions. Ref-MFC power production was not affected significantly until day 57th. After a transient condition that lasted for a few days, at day 67th Ref-MFC reached a new equilibrium state with an electric production ranging from 1.6 to 2.0 mW (average value of 1.8 ± 0.1 mW). Internal resistance showed instead a certain resilience to OLR variation and remained around values of 27–30 Ω. On the other hand, MPPT-MFC showed an immediate decrease of power production from 3.0 mW to 1.6 mW, to stabilize itself after day 58th to a value of 2.0 ± 0.1 mW. External resistance varied initially from 8 to 18 Ω; after day 64th it remained stable on 16.0 ± 2.4 Ω.

3.2. Electrochemical characterization

The electrochemical performances of both cells were assessed through polarization curves measurement.

These were performed once a week during the first experimental period for both MFCs, until the OLR variation was performed. Fig. 3 presents some of the most significant polarization curves.

Ref-MFC showed an OCV of 359 mV on day 7th, with a cathode Open Circuit Potential (OCP) of +86 mV vs SHE and an anode OCP of −274 mV vs SHE. The anode OCP value was close to the theoretical anode potential when acetate is oxidised to carbon dioxide ($E^{0\prime} = -284$ mV) [8]. The cathode OCP value, instead, was far below the theoretical cathode potential when oxygen is reduced to water ($E^{0\prime} = +816$ mV), but close to the redox potential of oxygen reduction to hydrogen peroxide ($E^{0\prime} = +257$ mV) [30,31]. This could indicate a partial accumulation of H_2O_2 in the catholyte.

After the first week the cathode OCP stabilized at lower values, ranging from 4 to 26 mV vs SHE, while the anode OCP decreased gradually until −366 mV vs SHE (day 35th). Maximum current intensity (in short circuit conditions, I_{SCC}) reached 27 mA on day 29th, when the cell internal resistance was at its measured minimum value of 12.4 Ω. The MPP reached its highest value, 2.2 mW, at the same occasion (with regards to the performed polarization curves). During all the start-up time OCV remained on values around 350 mV.

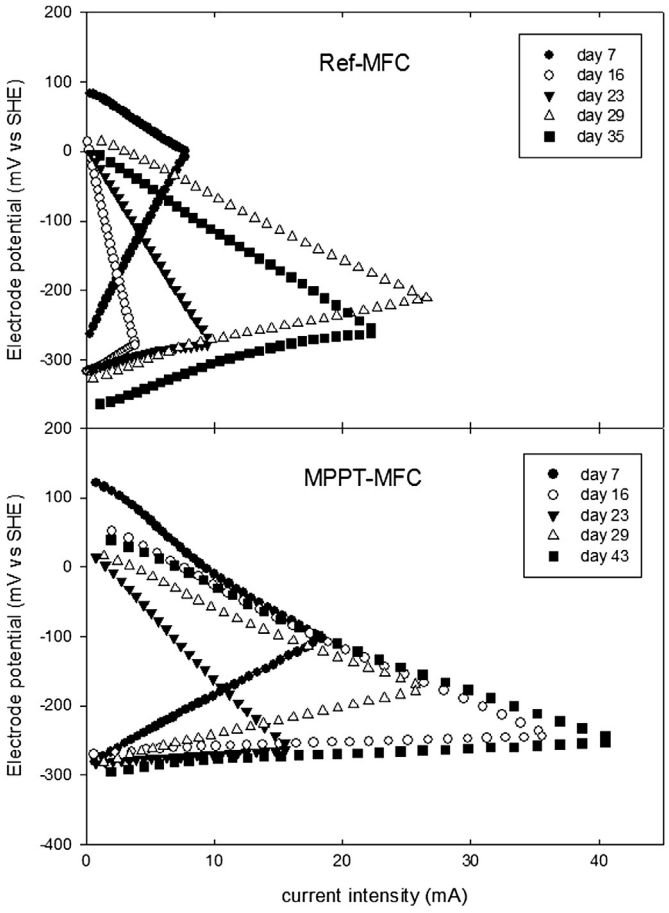

Fig. 3. Polarization curves of anode and cathode compartments, recorded during the first period for Ref-MFC and MPPT-MFC.

MPPT-MFC also showed a higher cathode OCP on day 7th (+125 mV vs SHE), value that than decreased to 22–62 mV vs SHE during the following weeks. These OCP values were again far below the redox potential corresponding to the complete oxygen reduction to water, and could be sign of an incomplete reduction to H_2O_2 [30]. The anode showed a stable behavior from the first polarization curve trial, with a mean OCP of −288 ± 9 mV vs SHE and low overpotentials, that made possible to reach an I_{SCC} of 42 mA and a MPP of 3.1 mW on day 43rd. The maximum values of I_{SCC} and MPP were reached meanwhile the internal resistance was at its minimum value (day 43rd, 8.6 Ω). The average value of OCV was 322 ± 15 mV, lower than that of Ref-MFC, while the measured cell voltage was 160 ± 26 mV (0.5 times the mean OCV). It can be easily demonstrated that the value 0.5 is typical of MFCs working at MPP condition [25].

3.3. Energy losses distribution

A more detailed analysis of the MFCs electrochemical behavior was provided by the calculation of the overpotentials related with the different components during the 2 main operational periods: first period, anode OLR at 10 kg COD m^{-3} d^{-1}; second period, anode OLR at 5 kg COD m^{-3} d^{-1}. Fig. 4 presents the energy losses distribution of Ref-MFC and MPPT-MFC treating swine wastewater. For this analysis, the transition data regarding the first days after inoculation and those collected immediately after OLR variation were not taken into account, as electrodes potentials were still

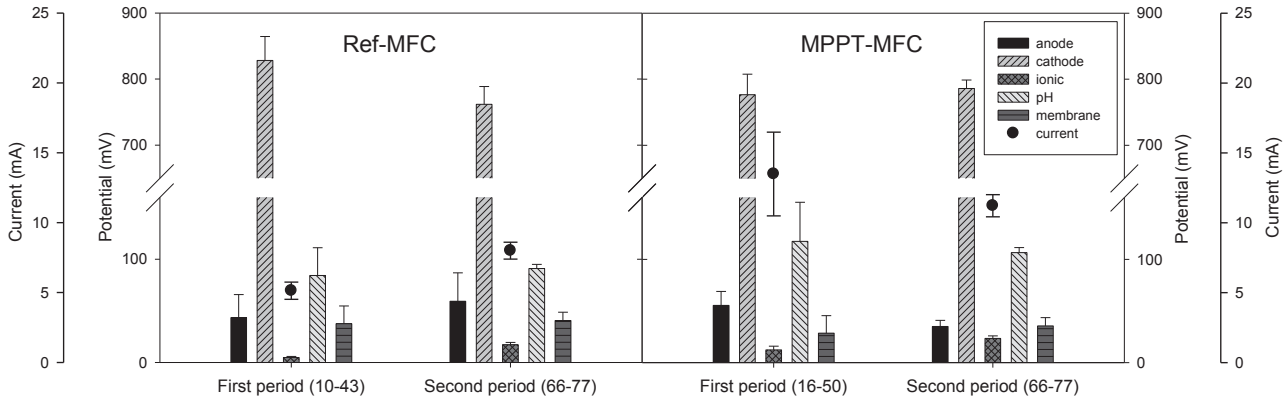

Fig. 4. Energy losses distribution for Ref-MFC and MPPT-MFC, calculated for the two experimental periods performed (within the days reported in parenthesis). Circled points indicate the mean current sourced by each MFC. Error bars represent standard deviations of replicate samples.

varying fast in time and the measurements were not representative of steady-state working cells [28].

It is reported that one way to minimize energy losses in MFCs is to operate them under optimal conditions for power production, at an optimal R_{ext} [18,32], but this subject was not fully explored in the literature.

Fig. 4 shows that, in relative terms, the main energy loss contribution in both MFCs was related with the cathode overpotential (about 80% of the total value). This was followed by the pH gradient loss (8–12%), the anode overpotential (4–6%) and the membrane transport loss (4%). The overpotential associated with the electrolytes (E_{ionic}) was negligible, due to their high conductivity. These relative energy loss contributions did not change significantly between the two MFCs and/or between the two experimental periods performed.

Taking into account also the current production, the MFCs energy losses were re-evaluated in terms of resistance. Each partial resistance contribution was calculated from the relative potential loss according to Ohm's law (data not shown). The total resistance was then calculated by summing all the partial terms.

In this way a difference between Ref-MFC and MPPT-MFC could be observed. In particular, the controlled cell showed a lower (total) resistance than the reference one, during the first experimental period (77 Ω vs. 198 Ω, meaning a 61% reduction). After the OLR variation the difference between the two MFCs became less visible, but MPPT-MFC still maintained a lower total resistance than Ref-MFC (88 Ω vs. 122 Ω, 28% reduction). Such resistance reduction surely meant a higher energy efficiency of the MPPT-MFC compared to the Ref-MFC, since with similar values of overpotentials the first cell was able to produce a higher current intensity.

3.4. Organic matter removal and Coulombic efficiency

Table 1 presents the average data of organic matter removal efficiency, current intensity and power, anode potential and Coulombic efficiency retrieved from Ref-MFC and MPPT-MFC before and after OLR variation. Again the data related to the first days after inoculation and those collected immediately after OLR variation were not taken into account in order to describe the behavior of the MFCs in (pseudo) steady-state conditions. However, slight differences in daily flow-rate and/or influent organic matter concentration, together with the periodic replacement of the whole swine wastewater laboratory stock, did not allow to have a perfectly stable organic loading rate. This affected in cascade the measurements of organic matter removal and Coulombic efficiency (as shown by the high values of standard deviations). Electrical performances seemed to be less affected.

Mean values of η_{COD} were not significantly affected by the application of the MPPT control system, but they only depended on the applied OLR. In particular, COD_t removal efficiency increased from 36–39% to 49–51% decreasing OLR from 10 to 5 kg COD m^{-3} d^{-1}.

Coulombic efficiency was calculated based on soluble COD and total BOD_5 removal, in order to take into account the filter-like behavior of the granular matrix filling the anode chamber, that could trap particulated organic matter and solids present in the swine wastewater (anode fuel). It was assumed that the real value of CE stayed within the interval of proposed values. Ref-MFC Coulombic efficiency increased from 6–7% to 10–11% moving from the first to the second experimental period. In the case of MPPT-MFC, CE remained around values of 15%. These values were coherent with the measurements of current intensity, since η_{COD} was almost equal for the two MFCs.

The electrical power did not follow the same behavior of current and/or CE. Meanwhile during the first period the behavior of the two cells was different, with a power produced by the MPPT-MFC more than two times higher than that of Ref-MFC, during the second observation period the performances were similar (mean power of 1.8–1.9 mW). Moreover, the power produced by MPPT-MFC did not seem to be affected by applied OLR. Instead, the observed anode potential was slightly affected by the OLR. It decreased of about 15 mV in both MFCs between the first and the second period. In the case of MPPT-MFC the anode exhibited a potential higher (less negative) and more stable than that of Ref-MFC.

4. Discussion

4.1. Effect of external resistance control on start-up time and anode biofilm growth

One of the main factors that delay peak performance and scaling-up of MFCs is the time required for the formation of an active exoelectrogenic biofilm at the anode electrode after inoculation [15]. Active external resistance control is supposed to be able to accelerate this biofilm growth and enrich exoelectrogenic cultures [10,11,15]. This study demonstrated that start-up time of MPPT-MFC was shorter than that of Ref-MFC, in line with previous experimental works addressed to the topic [7,10,11,15]. Indeed, the MFCs electric start-up finished when power production and internal resistance were constant in time. The MPPT system application drove the controlled cell to start-up in about 14 days. The fixed

Table 1
Comparison of organic loading rate (OLR), organic matter removal efficiency (η_{COD_t}), anode potential (E_{an}), current production (I_{mean}), power generation (P_{mean}) and Coulombic efficiency (CE) for Ref-MFC and MPPT-MFC, for the two experimental periods performed (within the days reported in parenthesis). CE values are calculated based on soluble COD removal (CE_{COD_s}) and total BOD_5 removal (CE_{BOD_t}). Error values represent standard deviations of replicate samples.

MFC	Experimental period	OLR (kg COD m^{-3} d^{-1})	η_{COD_t} (%)	E_{an} (mV vs SHE)	I_{mean} (mA)	P_{mean} (mW)	CE_{COD_s} (%)	CE_{BOD_t} (%)
Ref.	First (10–43)	10.5 ± 0.7	36 ± 18	−272 ± 21	5.0 ± 0.7	0.80 ± 0.21	6 ± 3	7 ± 3
Ref.	Second (66–77)	5.2 ± 0.1	49 ± 10	−287 ± 38	7.5 ± 0.4	1.77 ± 0.14	10 ± 2	11 ± 1
MPPT	First (16–50)	10.5 ± 0.7	39 ± 15	−250 ± 6	13.5 ± 3.0	1.94 ± 0.34	15 ± 7	18 ± 9
MPPT	Second (66–77)	5.2 ± 0.1	51 ± 5	−267 ± 4	11.2 ± 0.8	1.90 ± 0.09	14 ± 4	15 ± 1

resistance of Ref-MFC (30 Ω), although chosen as to match the internal resistance of the cell (in steady-state conditions), did not allow the system to start-up before day 43rd. At that day the internal and external resistances of Ref-MFC matched, and power generation started to increase until reaching values similar to that of MPPT-MFC. The start-up of Ref-MFC ended when the performances of both MFCs became comparable (around day 49th). Hence, automatic control of the external resistance contributed to reduce the MFC start-up procedure by about one month. This result is in agreement with similar experimental works [10,15] but this study was performed using real swine wastewater as anode fuel. The complexity of the wastewater surely influenced the acclimation time of the exoelectrogenic bacteria that colonized the anode compartments. This can explain the high start-up time showed by Ref-MFC. On the other hand, it demonstrates the efficiency of MPPT control and one advantage that could derive from its practical application on MFCs.

MPPT-MFC exoelectrogenic biofilm was stable after 2 weeks of continuous operation, as it is shown by the temporal power development (Fig. 2) and the anode polarization curves trend (Fig. 3). On the other hand, Ref-MFC showed unstable anode performances after one month of operation. Moreover, during the first experimental period, MPPT-MFC anode potential was stable around −250 mV vs SHE, compared to a more variable value of −272 ± 21 mV vs SHE for Ref-MFC (Table 1). The thermodynamic value for acetate oxidation (in pH-adjusted standard conditions) was equal to −284 mV vs SHE [8]. The more positive anode potential showed by MPPT-MFC could have increased the microorganisms energy yield per equivalent substrate oxidation [5,33], increasing also their bioelectrochemical activity and decreasing the start-up time needed by the cell. This result was demonstrated in previous studies [5,34] by poising the anode potential to both negative and positive values (vs SHE), but never by the application of an automatic control on the external resistance of the MFC. It can be supposed that the internal resistance of MPPT-MFC (and consequently the external resistance applied) was steadily on values lower than those of Ref-MFC. In this way, the exoelectrogenic bacteria of the MPPT-MFC anode could work at higher current demand regime and at less negative anode potential, gaining more energy for their growth and maintenance. Higher anode potential meant also less exploitable cell voltage, but this voltage deficit was absolutely overcome by the benefits in terms of biofilm growth and stability and, hence, current intensity produced (Table 1, Fig. 2).

These effects of MPPT control application on MFCs were still observable during the second experimental period, where internal resistance of MPPT-MFC was still half the value of Ref-MFC, and current intensity was 50% higher.

4.2. Short and long-term effect of external resistance control on Coulombic efficiency and power

Coulombic efficiency of MPPT-MFC was steadily higher than that of Ref-MFC but it did not change significantly decreasing the OLR from 10 to 5 kg COD m^{-3} d^{-1}, remaining on low values around 15%. This was probably due to the organic matter concentration (always higher than 1 g COD L^{-1}) that was not limiting the exoelectrogenic bacteria metabolism, but at the same time was favoring methanogenic activity [9]. On the other hand, Ref-MFC showed an increase in CE of 50–60% between the first and the second experimental period, reaching final values around 10–11%. This difference was due to the fact that Ref-MFC needed one month more to complete its start-up, and before the OLR variation was not working in optimal conditions. For the same reason, Ref-MFC power production increased from 0.8 to 1.8 mW between the first and the second period, whereas MPPT-MFC power remained quite stable on 1.9 mW. Comparing the data of the two MFCs related to the second experimental period, it could be estimated the effect of external resistance control on Coulombic efficiency: CE of MPPT-MFC was about 40% higher than that of Ref-MFC, meaning an increase of the anode biofilm biocatalytic activity [11,15]. This improvement was driven by the corresponding minimization of internal resistance, as explained in the previous Section 4.1. It demonstrates that a persistent optimal operation of the MFC at the MPP delivers to better performances, as the biofilm is continually selected for electrogenesis [11].

Low CEs in both MFCs were caused by the high OLR applied, with high possibility of side-reactions (such as methanogenesis and biofilm growth) [35]. The proportion of methane gas (v/v) in the headspace of the anode chambers, added to the dissolved part released through the anode effluent, was measured to be around 45% for Ref-MFC and 36% for MPPT-MFC (second period, data not shown). This might be attributable to the higher current production of MPPT-MFC compared to Ref-MFC. It demonstrated that R_{ext} control was able to enhance exoelectrogenic activity at the expense of methanogenesis. The result is in agreement with other experimental works [10,15]. On the other hand, Pinto et al. (2010) reported a half-saturation constant for exoelectrogenic bacteria growth equal to 20 $mg_{acetate}$ L^{-1}, compared to a value of 80 $mg_{acetate}$ L^{-1} for methanogens (using a Monod kinetic equation), confirming that a high substrate concentration favors methanogenic activity with respect to anode-respiring bacteria [9].

No significant differences in power production were observed after both MFCs were started-up: in terms of power density (calculated with respect to the net anodic volume) Ref-MFC produced 4.9 ± 0.4 W m^{-3} NAC, meanwhile MPPT-MFC reached 5.0 ± 0.2 W m^{-3} NAC. These results are comparable with that obtained by Freguia et al. (2007) on similar designed MFCs fed with acetate [36], and demonstrate the feasibility of using MFC technology to generate electricity while treating swine wastewater [19]. The results demonstrate also that MFCs power production in steady-state condition is not affected by the MPPT control system application, as far as a fixed external resistance near the optimal value (R_{int}) is chosen.

4.3. Effect of external resistance control on energy losses

In MFCs there are numerous internal resistance mechanisms that can diminish the potential use of the electron transfer to the

cathode via the anode [37]. One way to minimize these energy losses is to operate the MFC under optimal conditions for power production (MPP) at an optimal R_{ext} (equal to R_{int}) [18].

From the overpotentials analysis (Fig. 4), it appeared that almost 80% of the MFCs energy losses were related to the cathode reaction (hypothesizing complete reduction of oxygen to water). Besides the cathode compartments were inoculated together with the anodes at the beginning of the experiment, it can be reasonably assumed that the reduction reaction (in both MFCs) was unbiocatalyzed [36]. Cathode overpotential values may be lower assuming an incomplete oxygen reduction, with accumulation of hydrogen peroxide in the catholyte [30]. Indeed it was reported that carbon materials like granular graphite are good catalysts for H_2O_2 production reaction [31].

Energy losses related to the pH gradient between anode and cathode chambers represented the second entry of the balance, contributing up to 8–12% of the total value. This study tried to minimize the pH gradient losses adopting an anionic exchange membrane between anode and cathode, as to exploit the buffer effect of OH^- carriers like carbonate species [22]. The anode overpotential contributed only for 4–6% to the total energy loss. In accordance with other studies and with Section 4.1, this overpotential was associated with the energy required for the activation and maintenance of exoelectrogenic bacteria [38]. The membrane transport loss was minimized by the adoption of the anionic exchange membrane [27] and accounted as 4% of the total energy loss in both MFCs. Despite the maximal conductivities measured along the experiment were 2.7 mS cm^{-1} (for both anolyte and catholyte), ionic energy losses were negligible and represented less than 2% of the total loss [22].

These relative contributions (in terms of percentage) did not change significantly between the two MFCs.

Taking into account also the current production, instead, the effect of automatic resistance control application on the energy losses distribution could be observed and estimated in terms of resistance. The effect was far more evident during the first period but it was probably amplified by the incomplete start-up of Ref-MFC. Indeed, both overpotentials and the current sourced by MPPT-MFC did not change significantly between the first and the second period, showing how the cell performance was not limited by the applied OLR. Comparing the data of the two MFCs related to the second period, it could be observed how the total resistance of MPPT-MFC was 28% lower than that of Ref-MFC. This indicated a higher energy efficiency of MPPT-MFC with respect to Ref-MFC, because with similar values of overpotentials the first cell was able to produce a higher current intensity. In particular, the resistance associated with the anode was reduced of more than 50% by the application of MPPT control, demonstrating that anode biofilm catalytic activity was enhanced with the cell working at the MPP [9–11]. On the other hand, the resistance associated with the cathode decreased of 27% thanks to the control system adoption. Assuming an unbiocatalyzed cathode reaction, this could be explained by a more complete oxygen reduction to water, with less accumulation of H_2O_2 as intermediate product [30]. The remaining energy losses (ionic loss, pH gradient loss and membrane transport loss) were less influenced by the MPPT system application.

4.4. Perspectives

The study demonstrated that a MPPT control system was able to reduce MFC start-up time of about one month, and to follow its internal resistance fluctuations in time, as showed by the abrupt variation of OLR. Such advantage could be useful for continuous operations such as wastewater treatment, where influent quality varies over daily and seasonal basis. The application in real conditions, using swine wastewater as anode fuel, allowed to evaluate the control system from an inedited, industrial-oriented point of view. The reduction of start-up time and the increase of Coulombic efficiency certainly represented a step towards the industrialization and the practical applicability of MFCs. Treatment capacities up to 4 kg COD m^{-3} d^{-1}, coupled with a short hydraulic retention time of 5 h and a high anode OLR, confirmed the versatility of this technology with respect to wastewater depuration. Moreover, the increased current density allowed by MPPT control application drove to an increased amount of electrons available for the reduction reaction at the cathode. This would become widely interesting in case of exploitation of cathode reaction for novel contaminant removal technologies (such as nitrates, nitrites, sulphates, etc.).

Another interesting feature of the MPPT system was the online, real-time activity measurement of the exoelectrogenic biofilm operating at the MFC anode, achieved by the direct and easy monitoring of the internal resistance and power output variations [32]. This feature, common for all BESs (that were already proposed as process biosensors [39]) was enhanced by the real-time electrical optimization control and could be useful for WWTP operators, trying to rapidly adjust some operational parameters.

5. Conclusions

In this study a MPPT control system was used to maximize MFC power output and Coulombic efficiency, by matching R_{ext} and R_{int} values. A comparison between two replicate MFCs, one with MPPT control applied and one working with fixed resistance, was carried out. Swine wastewater was used as anode substrate. The study demonstrated that external resistance control was able to reduce MFC start-up time of about one month, and to minimize its internal resistance. Moreover, MPPT system increased exoelectrogenic activity and Coulombic efficiency of about 40%, limiting at the same time methanogenic activity in the anode chamber. Finally, MPPT control drove to 50% reduction of the energy loss related with anode oxidation, and to 27% reduction of the energy loss related with cathode reduction (both expressed in terms of resistance). Power production and organic matter removal were not affected by the control system application, after the start-up was finished. The development of the MPPT algorithm and its transfer to low cost and low power electronic devices could facilitate the overall MFC technology implementation into real-world applications such as wastewater treatment and bioenergy recovery.

Acknowledgments

This research was financially supported by the Spanish Government (CTQ 2011-23632). D. Molognoni was supported by a research grant from the Department of Electrical, Computer and Biomedical Engineering of the University of Pavia, and by a mobility grant from LLP/ERASMUS Programme. The authors wish to acknowledge Prof. Giuseppe Venchi and the staff of the Power Electronics Laboratory of the University of Pavia for their help in the design and implementation of the MPPT control system.

References

[1] K. Rabaey, W. Verstraete, Trends Biotechnol. 23 (2005) 291.
[2] R.A. Rozendal, H.V.M. Hamelers, K. Rabaey, J. Keller, C.J.N. Buisman, Trends Biotechnol. 26 (2008) 450.
[3] D. Pant, G. Van Bogaert, L. Diels, Bioresour. Technol. 101 (2010) 1533.
[4] J. Lobato, P. Cañizares, F.J. Fernández, M.A. Rodrigo, New Biotechnol. 29 (2012) 415.
[5] X. Wang, Y. Feng, N. Ren, H. Wang, H. Lee, N. Li, Q. Zhao, Electrochim. Acta 54 (2009) 1109.

[6] P. Aelterman, M. Versichele, M. Marzorati, N. Boon, W. Verstraete, Bioresour. Technol. 99 (2008) 8895.
[7] L. Woodward, M. Perrier, B. Srinivasan, AIChE J. 56 (2010) 2742.
[8] B.E. Logan, Microbial Fuel Cells, John Wiley & Sons, Inc., New Jersey, 2008.
[9] R.P. Pinto, B. Srinivasan, M.F. Manuel, B. Tartakovsky, Bioresour. Technol. 101 (2010) 5256.
[10] R.P. Pinto, B. Srinivasan, S.R. Guiot, B. Tartakovsky, Water Res. 45 (2011) 1571.
[11] G.C. Premier, J.R. Kim, I. Michie, R.M. Dinsdale, A.J. Guwy, J. Power Sources 196 (2011) 2013.
[12] L. Woodward, M. Perrier, B. Srinivasan, B. Tartakovsky, Biotechnol. Prog. 25 (2009).
[13] K.J. Chae, M.J. Choi, K.Y. Kim, F.F. Ajayi, W. Park, C.W. Kim, I.S. Kim, Bioresour. Technol. 101 (2010) 5350.
[14] N. Degrenne, F. Buret, B. Allard, P. Bevilacqua, J. Power Sources 205 (2012) 188.
[15] H.C. Boghani, J.R. Kim, R.M. Dinsdale, A.J. Guwy, G.C. Premier, Bioresour. Technol. 140 (2013) 277.
[16] P.C. Nien, C.Y. Lee, K.C. Ho, S.S. Adav, L. Liu, A. Wang, N. Ren, D.J. Lee, Bioresour. Technol. 102 (2011) 4742.
[17] J. Winfield, I. Ieropoulos, J. Greenman, J. Dennis, Bioelectrochemistry 81 (2011) 22.
[18] D.Y. Lyon, F. Buret, T.M. Vogel, J.M. Monier, Bioelectrochemistry 78 (2010) 2.
[19] B. Min, J. Kim, S. Oh, J.M. Regan, B.E. Logan, Water Res. 39 (2005) 4961.
[20] J.R. Kim, J. Dec, M.A. Bruns, B.E. Logan, Appl. Environ. Microbiol. 74 (2008) 2540.
[21] N. Pous, S. Puig, M. Coma, M.D. Balaguer, J. Colprim, J. Chem, Technol. Biotechnol. 88 (2013) 1690.
[22] S. Puig, M. Coma, J. Desloover, N. Boon, J. Colprim, M.D. Balaguer, Environ. Sci. Technol. 46 (2012) 2309.
[23] J. Kim, S. Cheng, S. Oh, B. Logan, Environ. Sci. Technol. 41 (2007) 1004.
[24] APHA, Am. Public Heal. Assoc., Washington, DC, USA, 2005.
[25] B.E. Logan, B. Hamelers, R. Rozendal, U. Schröder, J. Keller, S. Freguia, P. Aelterman, W. Verstraete, K. Rabaey, Environ. Sci. Technol. 40 (2006) 5181.
[26] Y. Fan, E. Sharbrough, H. Liu, Environ. Sci. Technol. 42 (2008) 8101.
[27] T.H.J.A. Sleutels, H.V.M. Hamelers, R.A. Rozendal, C.J.N. Buisman, Int. J. Hydrogen Energy 34 (2009) 3612.
[28] T.H.J.A. Sleutels, A. Ter Heijne, C.J.N. Buisman, H.V.M. Hamelers, Int. J. Hydrogen Energy 38 (2013) 7201.
[29] T.H.J.A. Sleutels, A. Ter Heijne, C.J.N. Buisman, H.V.M. Hamelers, ChemSusChem 5 (2012) 1012.
[30] F. Harnisch, U. Schröder, Chem. Soc. Rev. 39 (2010) 4433.
[31] R.A. Rozendal, E. Leone, J. Keller, K. Rabaey, Electrochem. Commun. 11 (2009) 1752.
[32] P. Clauwaert, P. Aelterman, T.H. Pham, L. De Schamphelaire, M. Carballa, K. Rabaey, W. Verstraete, Appl. Microbiol. Biotechnol. 79 (2008) 901.
[33] D.A. Finkelstein, L.M. Tender, J.G. Zeikus, Environ. Sci. Technol. 40 (2006) 6990.
[34] P. Aelterman, S. Freguia, J. Keller, W. Verstraete, K. Rabaey, Appl. Microbiol. Biotechnol. 78 (2008) 409.
[35] T.H.J.A. Sleutels, L. Darus, H.V.M. Hamelers, C.J.N. Buisman, Bioresour. Technol. 102 (2011) 11172.
[36] S. Freguia, K. Rabaey, Z. Yuan, J. Keller, Electrochim. Acta 53 (2007) 598.
[37] P. Liang, X. Huang, M.Z. Fan, X.X. Cao, C. Wang, Appl. Microbiol. Biotechnol. 77 (2007) 551.
[38] H.V.M. Hamelers, A. Ter Heijne, T.H.J.A. Sleutels, A.W. Jeremiasse, D.P.B.T.B. Strik, C.J.N. Buisman, Appl. Microbiol. Biotechnol. 85 (2010) 1673.
[39] B.H. Kim, I.S. Chang, G.C. Gil, H.S. Park, H.J. Kim, Biotechnol. Lett. 25 (2003) 541.